Journal Pre-proof

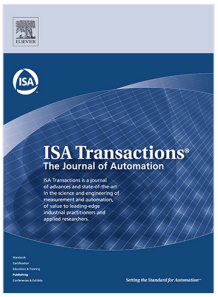

Load frequency control for multi-area power systems: A new type-2 fuzzy approach based on Levenberg–Marquardt algorithm

Ali Dokht Shakibjoo, Mohammad Moradzadeh, Seyed Zeinolabedin Moussavi, Ardashir Mohammadzadeh, Lieven Vandevelde

PII: S0019-0578(21)00193-2
DOI: https://doi.org/10.1016/j.isatra.2021.03.044
Reference: ISATRA 4054

To appear in: *ISA Transactions*

Received date : 2 October 2019
Revised date : 29 March 2021
Accepted date : 29 March 2021

Please cite this article as: A.D. Shakibjoo, M. Moradzadeh, S.Z. Moussavi et al., Load frequency control for multi-area power systems: A new type-2 fuzzy approach based on Levenberg–Marquardt algorithm. *ISA Transactions* (2021), doi: https://doi.org/10.1016/j.isatra.2021.03.044.

*Title page showing Author Details

Load Frequency Control for Multi-area Power System: a New Type-2 Fuzzy Approach based on Levenberg–Marquardt algorithm

Authors

Ali Dokht Shakibjoo
Ph.D. Candidate
Department of Electrical Engineering,
Shahid Rajaee Teacher Training University, Tehran, Iran
a.shakibjoo@sru.ac.ir

Mohammad Moradzadeh
Assistant Professor,
1- Department of Electrical Engineering,
Shahid Rajaee Teacher Training University, Tehran, Iran.
2- Department of Electromechanical,
Systems and Metal Engineering, Ghent University, Belgium,
Corresponding author: m.moradzadeh@sru.ac.ir, mohammad.moradzadeh@ugent.be

Seyed Zeinolabedin Moussavi
Associate Professor,
Department of Electrical Engineering,
Shahid Rajaee Teacher Training University, Tehran, Iran
smoussavi@sru.ac.ir

Ardashir Mohammadzadeh
Assistant Professor,
Department of electrical engineering,
East Azerbaijan province, University of Bonab, Iran
a.mzadeh@ubonab.ac.ir

Lieven Vandevelde
Professor,
Department of Electromechanical,
Systems and Metal Engineering, Ghent University, Belgium,
lieven.vandevelde@ugent.be

Load Frequency Control for Multi-area Power Systems: a New Type-2 Fuzzy Approach based on Levenberg–Marquardt Algorithm

Abstract

In this study, a new fuzzy approach is proposed for load frequency control (LFC) of a multi-area power system. The main control system is constructed by use of interval type-2 fuzzy inference systems (IT2FIS) and fractional-order calculus. In designing the controller, there is no need for the system dynamics, therefore the system Jacobian is obtained by a multilayer perceptron neural network (MLP-NN). Uncertainties are modeled by IT2FIS, and for training fuzzy parameters, Levenberg Marquardt algorithm (LMA) is used, which is faster and more robust than gradient descent algorithm (GDA). The system stability is studied by Matignon's stability method under time-varying disturbances. A comparison between the proposed controller with type-1 fuzzy controller on the New England 39-bus test system is also carried out. The simulations demonstrate the superiority of the designed controller.

Keywords: `Levenberg-Marquardt Algorithm, LFC, MLP-NN, Type-2 Fuzzy`

1. Introduction

The LFC problem is critical for the healthy operation of power systems. Keeping frequency at the rated value and tracking load changes on time, especially during dynamic changes of generation and consumption illustrates the importance of LFC. Preserving frequency of a system at a rated value after small-signal disturbances like load interruption, preserving the power exchange between the neighboring control areas in a large-scale system, and preserving

generation of each unit at a specific value are achieved via LFC in power system through the governor and the secondary control in case of larger disturbances.

Moreover, nowadays, renewable resources cause high fluctuations in power generation and frequency variation, considering the changes in the climate and the unknownness of the production rate. Considering the output uncertainty and intermittency of renewable resources, including the wind, the more use and influence of these resources can create a major challenge for frequency reliability and stability. Consequently, addressing this issue is essential to increase the influence rate of these resources in the network. In this regard, serious consideration is made towards the methods of frequency control and network stability. In addition to the influence of renewable resources, load changes cause changes and frequency fluctuations, where the power system is expected to remain stable after frequency stabilization. So far, various studies have been carried out on LFC [1–14].

The electric vehicles are used in [1] for LFC in a robust manner and proposed combined model of electric vehicles. With the advent of intelligent control, optimal responses were obtained with respect to conventional LFC. LFC with the intelligent PI is performed, using the genetic algorithm, bat algorithm, fuzzy logic, and artificial neural networks (ANN) by considering uncertainty and disturbances in [2–5]. A LFC with parametric and nonlinear uncertainty is examined in [2] and [3] by using adaptive fuzzy logic. A fuzzy control on the bases of bacterial tuning method is considered in [4] for designing LFC. Also, optimal PID is proposed in [5] by using a fuzzy differential algorithm.

Various fuzzy logic techniques have been studied for LFC in recent years [6, 7]. A straightforward and systematic method is developed in [6] to model the neural adaptive back-stepping control in chaotic systems with uncertainty by using the input-output data from the underlying dynamic systems. An adaptive approach is proposed in [8] to control the conventional PI and optimal LFC in which the control parameters in valid conditions by using a Sugeno-type fuzzy system. However, these conventional controllers, have some disadvantages; constant controllers are designed for normal operating conditions, and thus the

control performance decreases under variable operating conditions. Also, controllers like sliding mode controller cannot converge in a limited time and system parameters should be measured which degrades the control performance in complex systems with a variety of parameter estimations. Besides, in complex systems, the effect of chattering increases oscillation and instability of the system. Recently, a large number of studies have addressed the fractional-order PID (FOPID) due to its proper performance. This method is employed on various engineering and control problems [9–14]. Furthermore, different studies have been conducted to determine the FOPID parameters [15–22]. Recently, researchers have focused on using fuzzy logic controllers to improve the FOPID performance with fuzzy methods. As a result, satisfactory results were obtained from the FOPID application to nonlinear systems, which encouraged researchers to further use these controllers.

In our proposed control design, interval fractional-order type-2 fuzzy based on LMA (IT2FOFPID-LMA) is presented to LFC. Unlike previous studies, system dynamics are uncertain. The main controller is optimized by LMA. The robustness against uncertain parameters and independence to the plant model comparative the most important property of the proposed controllers. The proposed method is in the continuation of our previous works [23, 24] to improve the controller for controlling the frequency of a two-area system. In [23, 24], GDA was used for training and optimization. But slow speed requiring determining training rate and sensitivity to initial conditions are the shortcomings that motivated us to use LMA. Although other optimization methods based on the second-order Taylor series resolve problems of gradient descent, they require calculating the Hessian matrix. In addition, in our proposed method, the FOPID controller is used instead of conventional PID to improve performance. Due to presence of the FOPID, there are a large number of adjustable parameters; thus, LMA is used for optimization, which is more robust and faster compared to similar methods such as Newton-Gauss. In our proposed method, fuzzy neural networks (FNN) have been optimized using LMA showing better performance compared to error back-propagation based on gradient descent. The proposed

controller is compared with well-known controllers that are frequently used in the frequency regulation problem including PID and type-1 fuzzy inference system (T1FIS). Recently, various IT2FIS have been developed, but most of these controllers are designed for a particular case of nonlinear systems that it is difficult to be reformulated for our plant [25].

In the remaining, the motivation and main characteristics of the controller are presented in section 2. The controller theory and the method used to train the parameters are discussed in section 3. The suggested structure including MLP-NN, Jacobian and its training method are presented in section 4. Sections 5, 6 and 7 present system model, simulation and conclusion, respectively.

2. Motivation and main characteristics

The interconnected case study system includes different areas which are connected through high voltage transmission lines. LFC in each area not only controls frequency but also the power transfer between areas. Since frequency violations in power system affect performance, safety, reliability and efficiency of the power system and excess frequency violation degrades the power electronics equipment, resulting in overloaded transmission lines, LFC is important.

2.1. In terms of reliability

(1) The presence of renewable energy and load changes causes intense volatility in the actual power production of the power system. Considering equation of motion $2H\frac{d\Delta f}{dt}+D\Delta f=\Delta P_m-\Delta P_e$, a change in the power '$\Delta P_m-\Delta P_e$' leads to changes in the frequency and may result in inertial response.

(2) Uncertainty of the total generation because of increasing the generation capacity of renewable resources and establishing an imbalance between the mechanical power driving the generators and electrical power.

2.2. In terms of control for frequency stabilization

Regarding the uncertainty caused by fluctuations in renewable energy sources, including wind power, and in order to maintain frequency control, conventional

controllers fail to have a suitable performance against nondeterministic systems. Although features such as resistance to system gain changes and disturbance elimination are among the FO controller characteristics, which can distinguish them from conventional controllers, our proposed controller is used along with the IT2FIS to overcome the constraints, including uncertainly.

The main characteristics of this study are as follows:.

- The system is modeled with the MLP-NN.
- A LFC on the basis of IT2FOFPID-LMA is designed.
- Parameters of the controller are adjusted using IT2FIS and trained using LMA.
- Stability of the controller is studied using Matignon's stability theorem.
- The suggested controller is robust against time-varying disturbances.
- The proposed method is online, and adaptable that can adapt itself with the uncertain condition of the system.
- It is independent of system dynamics and its convergence speed is fast.
- It can be used in a system including nonlinearity, generation rate constraint and governor deadband.

In the following section, definitions and theories of FO, IT2FIS and LMA are presented first, and then, the proposed structure is described.

3. The Proposed theorem

3.1. Preliminaries

Conventional PID has three gains, but if it is considered to be FOPID, it becomes as represented in Eq. (1), having 5 degrees of freedom. Therefore,

FO is more efficient than the conventional PID controller and has thus become popular in the industry [26].

$$C(s) = k_p + k_i D_t^{-\alpha} e + k_d D_t^{\alpha} e \tag{1}$$

where D_t^{α} and $D_t^{-\alpha}$ are differentiator and integrator, t is limit of the operator and α is the FO. In addition, k_p, k_i and k_d are constants, $e = y - \hat{y}$ is the error signal and y, $\hat{y}$ are the desired value and estimated value, respectively. Operator D_t^{α} is defined as follows [27]:

$$D_t^{\alpha} = \begin{cases} \frac{d^{\alpha}}{dt^{\alpha}} & \alpha > 0 \\ 1 & \alpha = 0 \\ \int_a^t (d\tau)^{-\alpha} & \alpha < 0 \end{cases} \tag{2}$$

The details of Eq. (2) are given in [28–31]. Various definitions have been proposed for FO. The Caputo and RL are the most important definitions of FO integrator based on the combination of fractional-order integral and integer-order differentiation. The Caputo definition is more popular in practical applications, because, in this definition, the initial and boundary conditions have a physical concept [32]. In this paper, Caputo definition is given as [33]:

$$D_t^{\alpha} f(t) = \begin{cases} \frac{1}{\Gamma(m-\alpha)} \int_0^t \frac{f^{(m)}(\tau)}{(t-\tau)^{\alpha+1-m}} d\tau & m-1 < \alpha < m \\ \frac{d^m}{dt^m} f(t) & \alpha = m \end{cases} \tag{3}$$

Equation. (3) is adopted from the Cauchy formula in which m is the integer value and Γ represents Gamma function which is as follows [32]:

$$\Gamma(z) = \int_0^{\infty} t^{z-1} e^{-t} dt \tag{4}$$

Since the FO operator is of infinite dimension, it requires high order approximation with a limited frequency range. Various approximation methods for FO operator exists including Matsuda [32], Carlson [33] and Oustaloup [34].

Using the Caputo and RL definition to design a FOPID controller, the following integral operator is given for the FO integral:

$$ {}_{c}^{RL}I_{t}^{\alpha} f(t) = \frac{1}{\Gamma(\alpha)} \int_{c}^{t} \frac{f(\tau)}{(t-\tau)^{1-\alpha}} d\tau $$

for $m-1 < \alpha < m$.

Oustaloup approximation:

The filter is comprised of multiple compensators and has multiple poles and zeros around the frequency operating points, and it is one of the most well-known approximation methods [35]. In order to simulate and implement the method in MATLAB, the FO should be approximated with the integer-order. To this end, FO Modeling and Control (FOMCON) toolbox in MATLAB is used. Its transfer function s^{α} is defined as Eq. (5) [34–36]:

$$ s^{\alpha} = C_0 \prod_{k=1}^{N} \frac{s+\omega_{zn}}{s+\omega_{pn}} \tag{5} $$

where, C_0, ω_{zn} and ω_{pn} are gain, zero and pole and its value in the frequency range of ($\omega l \quad \omega h$) is [35]:

$$ \omega_{pn} = \omega_l \left(\frac{\omega_h}{\omega_l}\right)^{\frac{k+N+\frac{1+\alpha}{2}}{(2N+1)}} $$

$$ \omega_{zn} = \omega_l \left(\frac{\omega_h}{\omega_l}\right)^{\frac{k+N+\frac{1-\alpha}{2}}{(2N+1)}} \tag{6} $$

$$ C_0 = \omega_h^{\alpha} $$

where $(2N+1)$, represented filter order, ω_h/ω_b is upper/lower frequency band.

Proper performance of the FO controllers having more degrees of freedom has attracted attention in many applications in industry such as electrochemistry and electric circuits, and it is additionally combined with fuzzy logic to improve performance further. A large number of studies have investigated the performance of PID/FOPID in terms of reference tracking [13, 14]. Considering

the advantages of IT2FIS, this paper combines IT2FIS and FO controller for LFC to improve the overall performance.

3.2. IT2FIS Theory

In the design of LFC using control methods, efficiency and robustness should be balanced. The performance of simple classic controllers is not acceptable in the power system with nonlinear dynamics, uncertainties, variable and uncertain load. If the parameters of the LFC system are adjusted on the basis of classical trial-and-error approaches, its dynamic performance would be degraded in a wide range of performance and different load scenarios. Furthermore, the mathematical dynamics of the plant is not reliable in most of practical conditions. Accordingly, neuro-fuzzy approaches have been presented. But, these methods cannot withstand noise, uncertainty, and changes of parameters [37]. This study presented IT2FIS based controller. This controller performs better than T1FIS. The proposed controller is adaptive and can adapt to changes. The proposed controller is an improved development of the conventional PID and T1FIS [14]. Because of that, the performance is compared with these controllers. Furthermore, the PID and T1FIS are frequently used in the frequency regulation problem. Fuzzy systems are either type-1 or type-2 where in this paper, IT2FIS is used. The rules and membership function (MF) IT2FIS and T1FIS are considered to be same. But, T1FIS is not able to model uncertainties. The wide operational region, increased efficiency and reduced steady-state error and more uncertainty coverage are the reasons why IT2FIS is selected. IT2FIS was proposed by professor Zadeh in 1975 [38] in which, only type reduction block has been added. MF of the T1FIS is a crisp value. However, MF of IT2FIS, is fuzzy with two upper and lower MFs called $\bar{\mu}_{\tilde{\tilde{F}}}(x,u)$ and $\underline{\mu}_{\tilde{\tilde{F}}}(x,u)$, respectively.

$\tilde{\tilde{F}}$ is type-2 MF that is written as $\mu_{\tilde{\tilde{F}}}(x,u)$, where $x \in X, u \in J_x^u \subseteq [0,1]$ and $0 \leq \mu_{\tilde{\tilde{F}}}(x,u) \leq 1$ is defined in Eq. (7) [34]:

$$\tilde{\tilde{F}} = \left\{ (x, \mu_{\tilde{\tilde{F}}}(x)) | x \in X \right\} = \left\{ \int_{x \in X} \left[\int_{u \in J_x^u \subseteq [0,1]} \frac{f_x(u)}{u} \right] \Big/ x \right\} \tag{7}$$

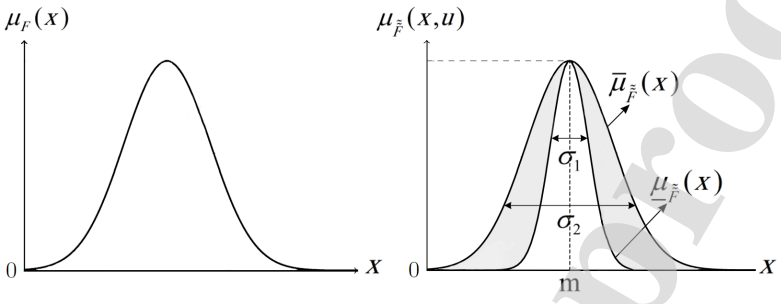

Figure 1: left) The T1FIS MF and right) IT2FIS MF with an uncertain deviation

As shown in Fig. 1, T1FIS includes no uncertainty, and for input, there exists a crisp value but in IT2FIS, there exists an interval for input, as shown in Fig. 1, which is obtained by shifting points of the Gaussian function to the left and right. There exists interval MFs for the input. Type-2 Gaussian function is described as follows [38]:

$$\mu_{\tilde{\tilde{F}}}(x,u) = \exp\left(-\frac{1}{2}(\frac{x-m}{\sigma})^2\right), \qquad m,\sigma = 1,2 \tag{8}$$

Here, m and σ represent the adjustable center and radius of the Gaussian function, respectively. The rules are: [39]

R^n: if x_1 is $\tilde{\tilde{F}}_{n1}$ and x_2 is $\tilde{\tilde{F}}_{n2}$, then y is Y

Where R^n is the MF of the n^{th} rule and x_1 and x_2 are inputs, and Y is the output parameter that is trained. There are various methods to reduce type, which has been mentioned in [39]. In this paper, the center-of-set (COS) method is used [40].

The structure of the IT2FIS is shown in Fig. 2 which includes five layers:

- Input layer: input of this layer is the output of the FO controller.
- Fuzzifier layer: converts crisp input to a fuzzy set. To reduce the uncertainties, measurement noise and disturbances are used.

- Fuzzy inference engine: this layer combined the fuzzy rules and the input fuzzy set is converted to the output one.
- Type reduction layer: to decrease the computational cost, T1FIS is used instead of IT2FIS.
- Defuzzifier layer: converts the fuzzy set to a crisp vector.

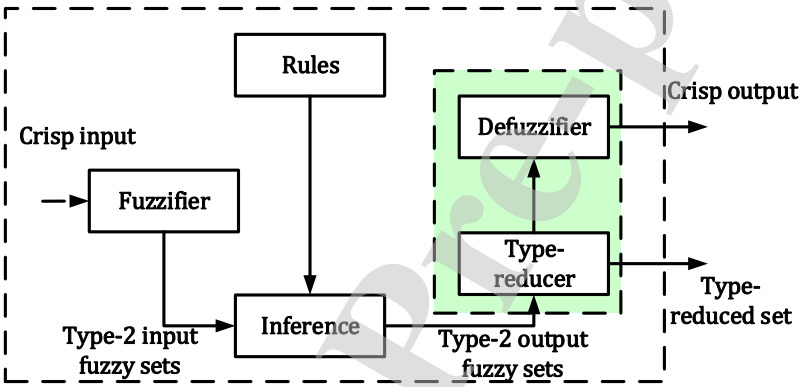

Figure 2: The block diagram of an IT2FIS [39]

This paper employs a IT2FIS and assumed the system dynamics to be uncertain. The IT2FIS can model more uncertainty compared to T1FIS; since it is adaptive; it can adapt itself to new conditions.

3.3. Levenberg–Marquardt Algorithm Theory

There are various methods for training the network among which gradient descent and Levenberg–Marquardt (LM) are the most well-known and applicable ones. A back-propagation method using gradient descent approach is employed to reduce the squared error between the reference and target outputs, and LMA is used in the optimization of nonlinear functions. LMA is a combination of gradient descent and Newton-Gauss for reducing error. As the value of the parameter gets far from its optimal value, gradient descent operates, and when

it is close to the optimal value, the Newton-Gauss method operates. Gradient descent is slow but with stable convergence. The Newton-Gauss method has a high convergence rate, which can resolve slow convergence of the gradient descent [41]. Therefore, these two methods are combined as the most efficient and fastest training method, which is used in this paper. Although this combined method is slower than the Newton-Gauss method, it is faster than gradient descent. Solving nonlinear regression problems and finding minimum optimal of square functions $F(x_0, x_1, ..., x_N) = \Sigma_{i=0}^{M} f_i^2(x_0, x_1, ..., x_N)$ is one of the most important application of LM method. LM is more robust than GDA and it can converge to the global minimum by selecting arbitrary initial conditions despite having several minimums [42]. In this paper, considering the advantages of LMA and drawbacks of error back-propagation based on gradient descent [43], LMA is used to increase convergence rate, reliability, and robustness of the controller.

4. Structure of the Proposed Method

The MLP-NN is used for model estimation. Simplicity and good estimation accuracy are the features of MLP-NN. The bipolar sigmoid activation function is used for neurons of the middle layer and the gradient descent technique is used for tuning the weights of MLP-NN. Section 4.1. describes details of the model. For activation function of the IT2FIS, Gaussian MF is used. The weights are trained using the LMA which converges better compared to similar methods such as Newton and it is trained such that our objective that is making frequency changes zero, is realized. To reduce the system type, the COS method is selected. The controller weights are trained adaptively and online which increases speed and enhances the performance of the controller. Also, the FO structure is used considering its more degrees of freedom compared to the conventional controllers that increase performance of the system. Details of the structure are presented in the subsequent sections.

Following, the designed control strategy is illustrated. The schemed control is depicted in Fig.3. The main idea is that FNN parameters are tuned so that

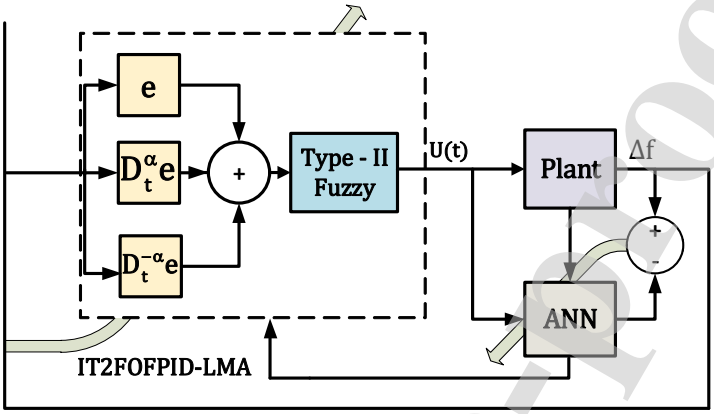

Figure 3: The proposed control structure

frequency deviation is converted to zero level. Following, the tuning laws of FNN are illustrated.

4.1. Structure of the MLP-NN

In this paper, a simple MLP-NN is used for online modeling of the plant. In recent years some new methods have been presented for online estimation time-varying nonlinear systems such as time-delay neural network [44] and fuzzy controller [45]. MLP-NN is used to model the system which employs the approximated model to obtain system Jacobian. In Fig. 4, $u(t-z_i), \quad i=1,..,n$ are inputs of ANN and z_i represents delay.

$w_{11}^1, w_{12}^2, ..., w_{1n}^1$; are the corresponding parameters of the first neuron in hidden layer.

$w_{21}^1, w_{22}^1, ..., w_{2n}^1$; are the corresponding parameters of the second neuron in hidden layer.

$w_{h1}^1, w_{h2}^1, ..., w_{hn}^1$; are the corresponding parameters of the h^{th} neuron in hidden layer.

$w_{21}, w_{22}, ..., w_{2h}$; are the corresponding parameters of the output.

The output of the suggested ANN is written as (see Fig.4):

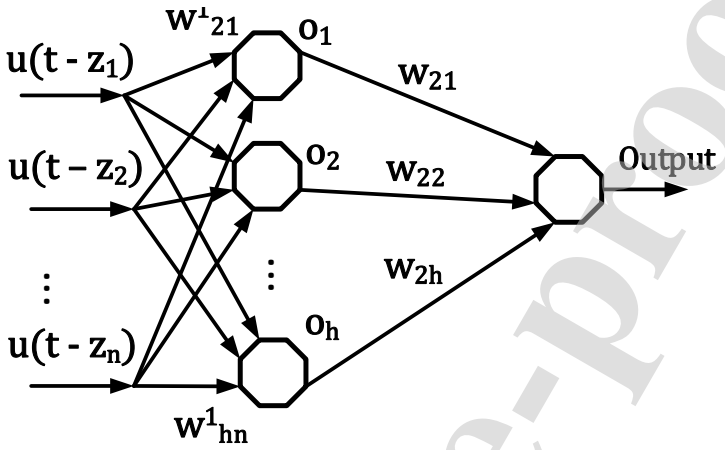

Figure 4: MLP-NN structure for system modeling

$$n_{ti} = w_i^1 U$$

$$o_i = g(n_{ti}), i = 1, ..., h \tag{9}$$

where,

$$w_i^1 = [w_{i1}^1, w_{i2}^1, ..., w_{in}^1] \tag{10}$$

$$g(n_{ti}) = \frac{1 - \exp(-n_{ti})}{1 + \exp(-n_{ti})}$$

The output of the ANN 'y' would be as:

$$y = w_2 o \tag{11}$$

where,

$$o = [o_1, o_2, ..., o_h]^T$$

$$w_2 = [w_{21}, w_{22}, ..., w_{2h}] \tag{12}$$

The parameters of this ANN are tuned considering:

$$E = \frac{1}{2}e_{est}^2 = \frac{1}{2}(y_d - y)^2 \tag{13}$$

where y/y_d represent the real/estimated outputs. The updating law is:

$$w_2(t+1) = w_2(t) + \eta e_{est} o \tag{14}$$

Weights adaptive law of the first layer is:

$$w_i^1(t+1) = w_i^1(t) + \eta e_{est} \dot{g}(n_{ti}) w_{2i} U \tag{15}$$

where w_i^1 is the vector of weights for i^{th} neuron. w_{2i} is the vector of weights for i^{th} neuron in the output layer. $\dot{g}(n_{ti})$ is the differentiation of $g(n_{ti})$ with respect to the input n_{ti} . η is constant.

4.2. System Jacobian

After obtaining the model, the system Jacobian is calculated as follows:

$$\frac{\partial \Delta f}{\partial u_c} = \left([w_{11}^1, w_{21}^1, ..., w_{h1}^1] diag[\dot{g}(n_{t1}), ..., \dot{g}(n_{th})] w_2 \right) \tag{16}$$

4.3. Suggested IT2FIS

The structure of the IT2FIS is presented in Fig. 5. M represents number of rules, and number of inputs of the network which is assumed to be 3 [38, 46].

Forward output of the controller is obtained using the following steps:

- Firing fuzzy rules are as Eq. (18):

$$\bar{\mu}_{\tilde{F}}(x, u) = \exp(-\frac{||X - C_k||^2}{\bar{\sigma}_k^2}) \tag{17}$$

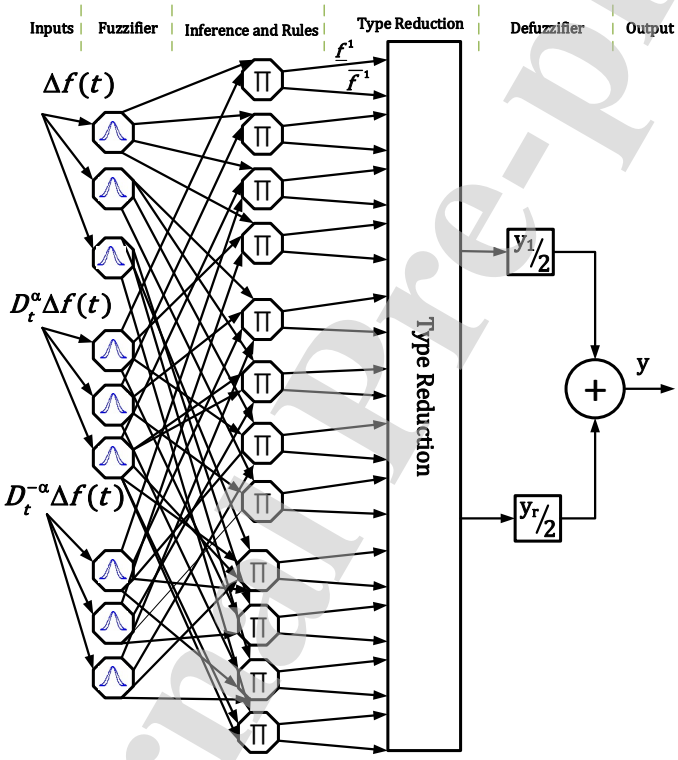

Figure 5: IT2FIS structure [42].

$$\underline{\mu}_{\tilde{F}}(x,u) = \exp(-\frac{||X - C_k||^2}{\underline{\sigma}_k^2}) \tag{18}$$

$$k = 1, ..., M$$

where, $X(t) = (\Delta f(t), D_t^{\alpha}\Delta f(t), D_t^{-\alpha})^T$ is the input vector and σ_i and C_i are width and center of the Gaussian function.

- The fuzzy system Output 'u_c' based on COS order-reduction is as Eq. (19) [36]:

$$y_{l,r} = \begin{cases} y_l = \frac{\sum_{n=1}^{L} \bar{f}^n \underline{y}^n}{\sum_{n=1}^{L} \bar{f}^n + \sum_{n=L+1}^{N} \underline{f}^n} + \frac{\sum_{n=L+1}^{N} \bar{f}^n \underline{y}^n}{\sum_{n=1}^{L} \bar{f}^n + \sum_{n=L+1}^{N} \underline{f}^n} \\ y_r = \frac{\sum_{n=1}^{R} \underline{f}^n \bar{y}^n}{\sum_{n=1}^{R} \underline{f}^n + \sum_{n=R+1}^{N} \bar{f}^n} + \frac{\sum_{n=R+1}^{N} \underline{f}^n \bar{y}^n}{\sum_{n=1}^{R} \underline{f}^n + \sum_{n=R+1}^{N} \bar{f}^n} \end{cases} \tag{19}$$

where, $\bar{f}_n, \underline{f}_n$ are the firing levels, and $\bar{y}_n$, $\underline{y}_n$ are the consequent output, and N is the rules number. The numerical output (crisp) of the IT2FIS is as follows:

$$y = \frac{y_l + y_r}{2} \tag{20}$$

4.4. Learning based on Error Back-Propagation and Levenberg–Marquardt for the Fuzzy Controller

This section describes tuning on bases of LMA. For initiation, the cost function is considered to be:

$$E = \frac{1}{2}e^2 = \frac{1}{2}(\Delta f)^2 \tag{21}$$

In order to train the fuzzy system, LMA is used. LMA is similar to the Newton-Gauss method, and does not require calculating the Hessian matrix, and it's benefits from the high-speed feature of the second-order methods. The Hessian matrix is written as Eq. (22) [41]:

$$H = J^T J \tag{22}$$

And the gradient is calculated as follows:

$$g = J^T e \tag{23}$$

where J denotes the Jacobian matrix. The LMA employs the following procedure described by Eqs. (24-27) to approximate the Hessian matrix.

$$Q(k) = (J^T J + \mu I)^{-1} \tag{24}$$

Therefore, the algorithm used to adjust the weights (rules parameters) would be as follows:

$$\omega_{t+1} = \omega_t - (J_t^T J_t + \mu I)^{-1} J_t e \tag{25}$$

I represents the identity matrix, μ is a combination coefficient.

Equation (25) is converted to Newton-Gauss for small values of μ as Eq. (26).

$$\omega_{t+1} = \omega_t - (J_t^T J_t)^{-1} J_t e \tag{26}$$

and it is converted to gradient descent for large values of μ as Eq. (27):

$$\omega_{t+1} = \omega_t - \alpha g_t \tag{27}$$

where $\alpha = \frac{1}{\mu}$.

Equation. (25) is rewritten as in Eq. (28) to guarantee that the calculation is stabilized.

$$w_{t+1} - w_t = -[J^T J + \mu diag(J^T J)]^{-1} J_t e \tag{28}$$

A solution has been presented by Jupp and Vozoff (1975) to enhance stability. In this solution, the algorithm is modified by singular value decomposition (SVD). SVD is used to divide a matrix of dimension $M \times N$ into three arbitrary matrices with the following relationship:

$$J = USV^T \tag{29}$$

where U is a matrix of dimension $M \times N$ which is an eigenvector from data, V is a $N \times N$ matrix from parameter space, and S is $N \times N$ diagonal matrix representing the square root of J.

$$S = diag(\sigma_1, \sigma_2, ..., \sigma_i), \quad \sigma_1 \geq \sigma_2 \geq ...\sigma_i \tag{30}$$

Reference [47] has used a $N \times N$ diagonal matrix P which its components are defined in Eq. (31) to define the damping parameter in LMA.

$$P_i = \frac{z_i^{2H}}{z_i^{2H} + \lambda^{2H}} \tag{31}$$

where z_i is a ratio between the diagonal elements of S , H is an integer defined as 2 in the algorithm and λ is error level which is user-defined and should be selected as large value that decreases as the solutions model's error decreases at every iteration. The modified solution of LMA using SVD as in Eq. (32) is obtained using the damping matrix as follows:

$$\Delta w = VPS^{+}U^{T}e \tag{32}$$

where S^{+} is $N \times N$ matrix with $\frac{1}{S_i}, (i = 1, 2, ..., N)$ as its component values [47].

LMA steps are represented in a flowchart shown in Fig. 6 [41]. E_t is the sum of squared error.

In order to find $\frac{\partial \Delta f}{\partial \Delta w}$, chain differentiation is used as:

$$J = \frac{\partial \Delta f}{\partial u_c} \frac{\partial u_c}{\partial y} \frac{\partial y}{\partial w} \tag{33}$$

where y is output of the ANN, u_c is the control signal, and $\frac{\partial \Delta f}{\partial \Delta u_c}$ is the system Jacobian is obtained from Eq. (16), and:

$$E = \frac{1}{2}e^2 = \frac{1}{2}(\Delta f)^2 \Rightarrow \frac{\partial E}{\partial \Delta f} = \Delta f$$

$$u_c = y \Rightarrow \frac{\partial u_c}{\partial y} = 1 \tag{34}$$

$$y = w^T \xi \Rightarrow \frac{\partial y}{\partial w} = \xi$$

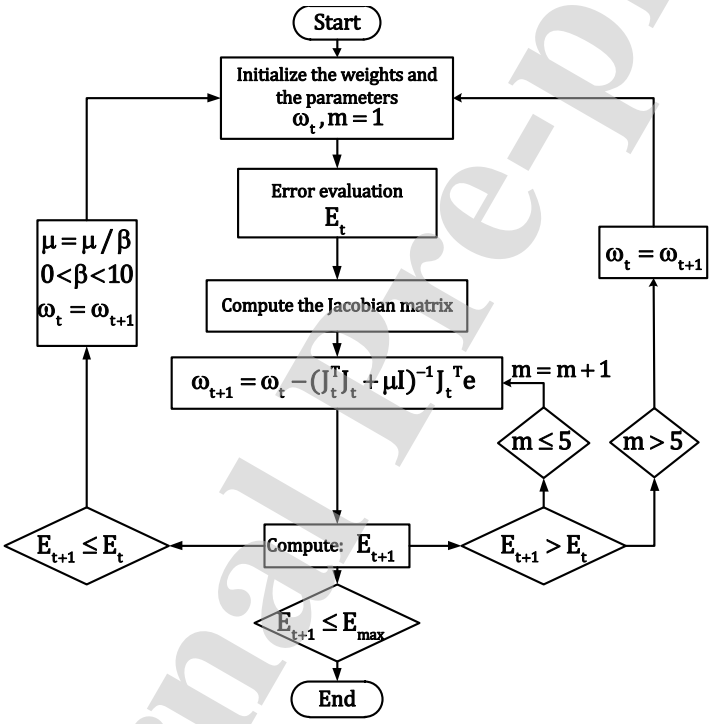

Figure 6: Levenberg-Marquardt algorithm flowchart [41]

In order to study stability, considered the following for:

$$D_t^{\alpha} x(t) = Ax(t) + Bu(t) \tag{35}$$

$$y(t) = Cx(t)$$

where, $u \in R^r$, $x \in R^n$ and $y \in R^P$ are input, state vectors and system output.

Equation (35) with $(0 < \alpha < 1)$ is stable if Matignon stability criterias are satisfied [30]

According to Matignon stability theory, the sufficient and necessary condition for stability of $H(s) = \frac{Z(s)}{P(s)}$ is as follows:

$$|arg(eig(A))| > \frac{\alpha}{\frac{\pi}{2}} \tag{36}$$

where eig(A) is eigenvalues of matrix A.

When $\sigma = 0$, the system is unstable and if $\alpha = 1$, according to the classic control theory, the system pole lies on the left side of the imaginary plane and it is stable.

Lemma: consider the FO system as Eq. (37) [27]:

$$D_{\omega}^{\alpha} = f(\omega) \tag{37}$$

where $0 < \sigma < 1$ and $\omega \in R^n$. By solving $f(\omega) = 0$, equilibrium points of α are calculated.

The stability of equilibrium points are ensured if eigenvalues of $\lambda_j, (j = 1, 2, ..., n)$ meet the below conditions :

$$|\arg(eig(J))| = |\arg(\lambda_j)| > \alpha\frac{\pi}{2}, \quad j = 1, 2, ..., n \tag{38}$$

where $J = \frac{\partial f}{\partial w}$ is the Jacobian matrix and n is the maximum number of poles p_i.

According to the given lemma and stable relationship in Eq. (38), if poles of the system are inside the stability area in Fig. 7, the closed-loop system is stable.

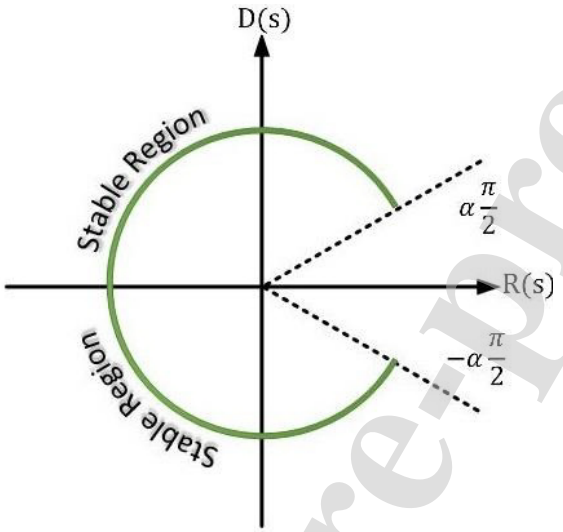

Figure 7: Stable region illustration for commensurate-order systems

On the other hand, eigenvalues of Jacobian of the closed-loop system satisfy the mentioned conditions in Eq. (38), and the closed-loop stability diagram shows that the system is stable.

5. Model of the Studied System

The suggested controller is tested on a power system with two-areas. Figure. 8 represents a schematic of the two-area power system. The system includes two LFC areas with several generators in each area. All generators of an area are represented by an equivalent generator. Each area has a number of re-heated steam turbines. In a system with multi-areas, besides adjusting frequency in the same area, the power between areas should be adjusted at a predetermined value; in other words, ΔP_{tie} should be very small or zero so that economic power distribution is observed. Then for stabilization, an area control error (ACE) signal is used which is the power difference between area load and

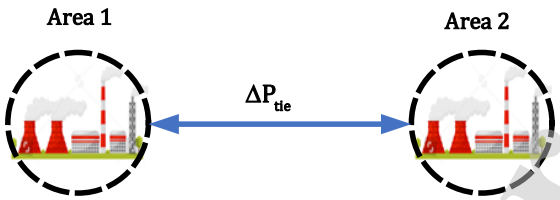

Figure 8: Block diagram of a power system with two-area

generation defined as for the control area i as follows:

$$ACE_i = \Delta P_{tie} + \beta_i \Delta f_i, i = 1, 2$$

Dynamic equations of frequency changes are as follow [23]:

$$\Delta \dot{f}_i = -\frac{1}{T_{Pi}}\Big(\Delta f_i + K_{Pi}(\Delta P_{tie,i} + \Delta P_{Gi} + \Delta P_{Di})\Big) + \frac{1}{T_{Gi}}\Delta P_{Ci} \tag{39}$$

Dynamics of the turbine are described as follows:

$$\Delta \dot{P}_{Gi} = -\frac{1}{T_{Ti}}(\Delta P_{Gi} + \Delta P_{Ri}) \tag{40}$$

Dynamic of the re-heated turbine is described in Eq. (41):

$$\Delta \dot{P}_{Ri} = -\frac{1}{T_{Gi}R_i}(\Delta f_i + K_{Ri}R_i\Delta X_{Gi}) + \frac{1}{T_{Ri}}(\Delta X_{Gi} - \Delta P_{Ri}) \tag{41}$$

The power exchange between areas i and j is:

$$\Delta \dot{P}_{tie}^{ij} = K_{Sij}(\Delta f_i - \Delta f_j) \tag{42}$$

Parameters and variables are listed in Table 1.

Remark 1:

It's worth to mention that to simplify the implementation of the fuzzy-based controller, the rule database and structure in our suggested method are fixed.

Table 1: Power system parameters for i^{th} area

Parameters	Description
$\Delta f_i(t)$	Frequency deviation
$\Delta X_{Gi}(t)$	Governor valve position
$\Delta P_{Di}(t)$	Load disturbance
$\Delta P_{tie,i}(t)$	Tie-line power flow
$\Delta P_{Gi}(t)$	Generator output power
ACE_i	Area control error
R_i	Drooping characteristic
K_{Ri}	Re-heat turbine gain
K_{Pi}	Power system gain
T_{Ri}	Re-heat turbine time constant
T_{Ti}	Turbine time constant
T_{Pi}	Power system time constant
K_{Sij}	Interconnection gain between control areas
T_{Gi}	Thermal governor time constant
β_i	Frequency bias factor

To improve the estimation performance, some self-structuring fuzzy systems have been introduced [48]. For future studies, the suggested controller can be developed by the use of self-structuring fuzzy systems.

6. Simulation Results

This section investigates the proposed controller's performance using simulations. The test system is a re-heated two-area power system shown in Fig. 9. This structure is comprised of two layers using sigmoid activation function. A set of 15 fuzzy rules is used to map the input variables for applying the fuzzy logic to each area. The number of rules is 9. A back-propagation algorithm based on gradient descent method is used to train the network. The PID controller is tuned via trial and error. The designed control method is compared

with internal model control based PID (IMC-PID). A second-order model is employed to approximate the transfer function of power system. The process of tuning the IMC-PID is given in the following [49, 50]: The system model is split in two parts:

$$\Omega(s) = \Omega_a(s)\Omega_b(s)$$

where Ω_a indicates the minimum phase, and Ω_b indicates the non-minimum phase. IMC controller is written as:

$$\Phi_a(s) = \Omega_a^{-1} \times \frac{1}{(\alpha s + 1)^n}$$

where α represents an adjustable parameter and n shows the degree of Ω_a.

Then IMC control scheme for rejecting disturbance is written as:

$$\Phi_b(s) = \frac{\theta_1(s) + \theta_2 s + ... + \theta_m s + 1}{(\beta(s) + 1)^m}$$

where β is the disturbance rejection parameter, m represents the number of poles of Ω and θ_1, θ_2, ..., θ_m should meet the following:

$$(1 - \Omega(s))(\Phi_a(s)\Phi_b(s))|_{s=0}$$

The following is used to obtain the feedback controller:

$$M(s) = \frac{\Phi_a(s)\Phi_b(s)}{1 - \Omega(s)\Phi_a(s)\Phi_b(s)}$$

The PID parameters are adjusted using the Maclaurin series and extending $M(s)$. To compare the proposed controller with IT2FPID based on GDA (IT2FPID-GDA) and other controllers fairly, IT2FOFPID-LMA controller is optimized in the same condition. For IT2FOFPID-LMA the best gains are derived as $K_p = 10$, $K_i = 10$, $K_d = 10$, $\alpha = 0.5$ for areas 1,2. Also, the width of the Gaussian function are considered $\bar{\sigma} = 10$, $\underline{\sigma} = 1$, respectively. The gains of IMC-PID and PID are given in Table 2.

The description of simulation conditions is provided in Table 3. The proposed method is further compared with some well-known controllers that are

Table 2: Controller Parameters

Area	IMC-PID	PID
1	K_p=4.80, K_i=6.30, K_d=1.440	K_p=2.370, K_i=0.680, K_d=0.170
2	K_p=7.40, K_i=9.10, K_d=2.50	K_p=1.990, K_i=0.759, K_d=0.186

frequently used in the frequency regulation problem such as PID and IT2FIS. To study the robustness, two cases are considered for simulations. Also, the error integral criteria is used for evaluation.

Table 3: Nominal parameter of power system

Parameters	Value
T_{Ti}	0.30 s
T_{Pi}	20 s
T_{Ri}	10 s
T_{Gi}	0.080 s
β_i	0.425 p.u.MW/Hz
K_{sij}	0.545 p.u/MW
R_i	2.40 Hz/p.u.MW
K_{Pi}	120 Hz/p.u

Case 1: In case 1, time-varying disturbance as $\Delta P_D = |sin(t)|$ is considered in both areas of the system. Frequency changes and control trajectorys of the closed-loop system with IT2FPID-GDA, IT2FOFPID-LMA and PID in areas 1 and 2 are depicted in Figs. 10-12.

We see that our proposed method, IT2FOFPID-LMA, yields better transient response and stability compared to other methods; in other words, it has a shorter settling time. Furthermore, oscillation in our proposed method of IT2FOFPID-LMA becomes stable after 30s while in other methods, oscillations of the control trajectory continue.

Case 2: In this case, the time-varying disturbance is not considered at the system output. Frequency changes in areas 1 and 2 with IT2FPID-GDA,

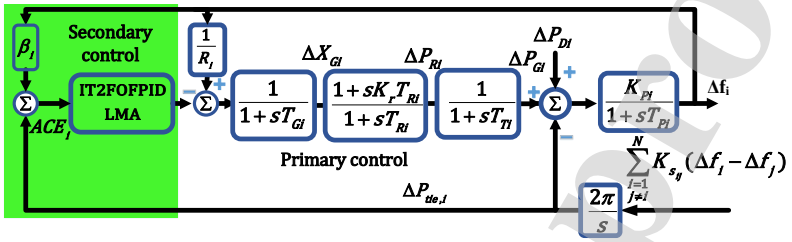

Figure 9: Multi-area LFC with the proposed controller

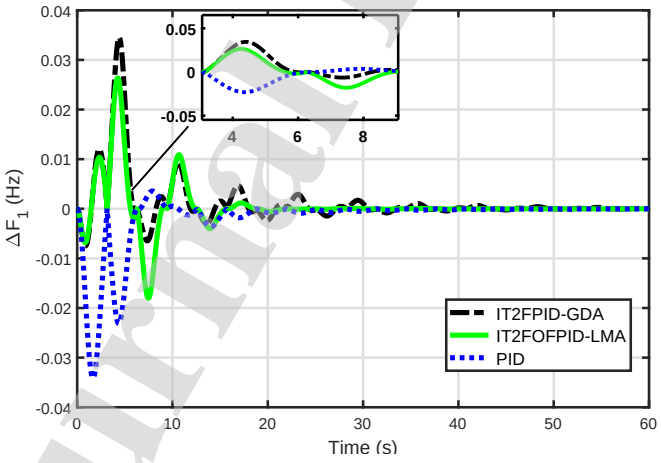

Figure 10: Case 1: Frequency changes with disturbance; area 1

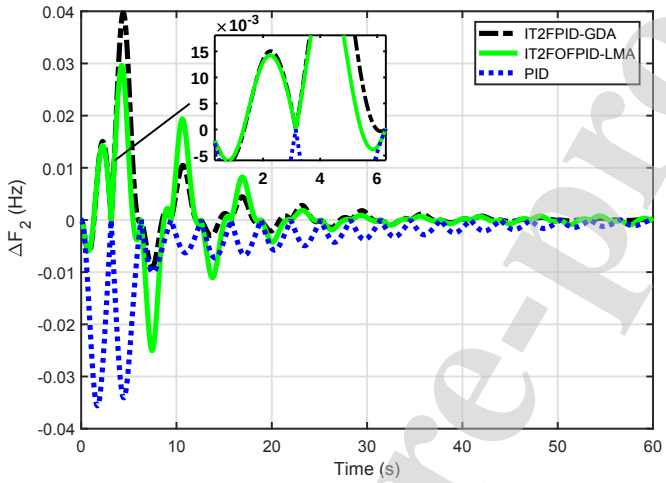

Figure 11: Case 1: Frequency changes with disturbance; area 2

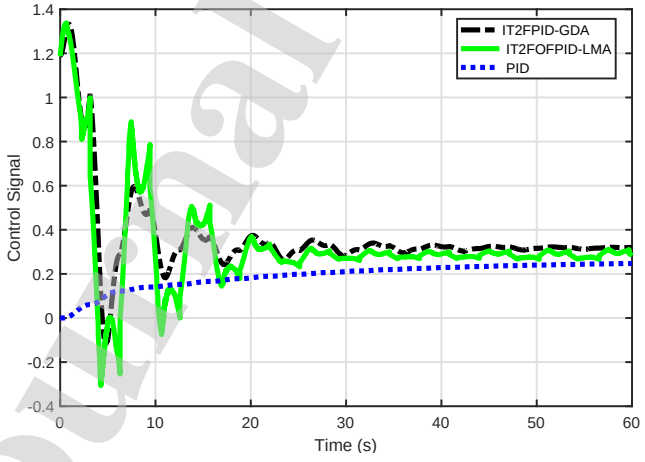

Figure 12: Case 1: Control trajectory with disturbance; area 1

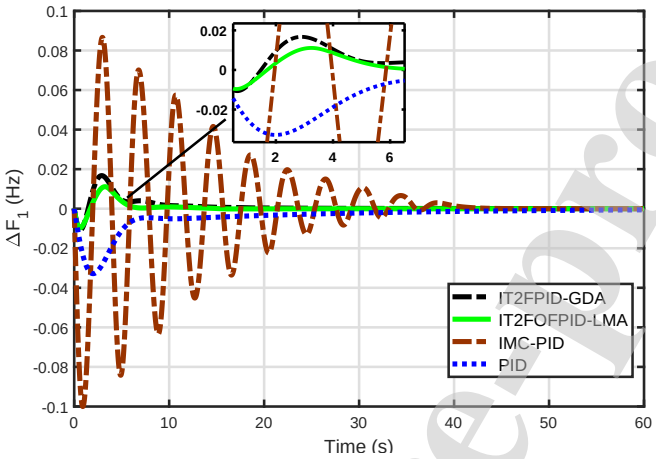

Figure 13: Case 2: Frequency changes without disturbance; area 1

IT2FOFPID-LMA, PID and IMC-PID are shown in Figs. 13 and 14. We see that in our proposed method, frequency oscillations have 10% overshoot and become stable after 8s which is better than other controllers. This indicates the superiority of our proposed method, which becomes stable with a quick and small oscillation.

Moreover, the control trajectory of areas 1 and 2 are shown in Figs. 15 and 16, respectively. We see that the control trajectory of our proposed method in both areas becomes stable without any oscillations, while changes of control signal of the other controllers are oscillatory.

Changes of the power exchange between areas 'ΔP_{tie}' in cases 1 and 2 are shown in Figs. 17 and 18, respectively. We see that ΔP_{tie} our proposed controller stabilizes smoothly without any oscillations but it oscillates in other control methods.

To evaluate the robustness, error integral criteria is used. The evaluation indexes are defined as:

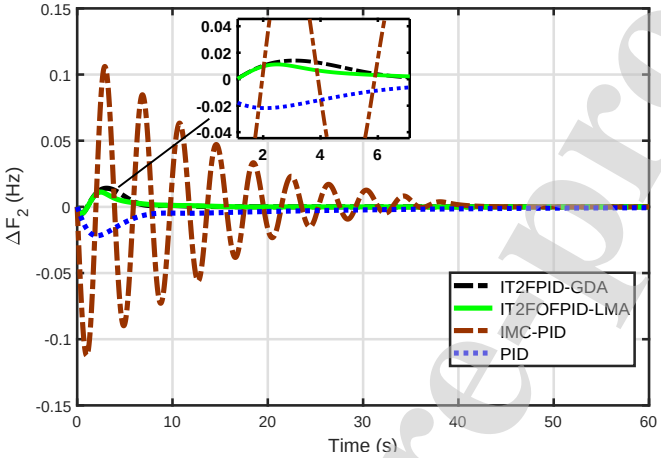

Figure 14: Case 2: Frequency changes without disturbance; area 2

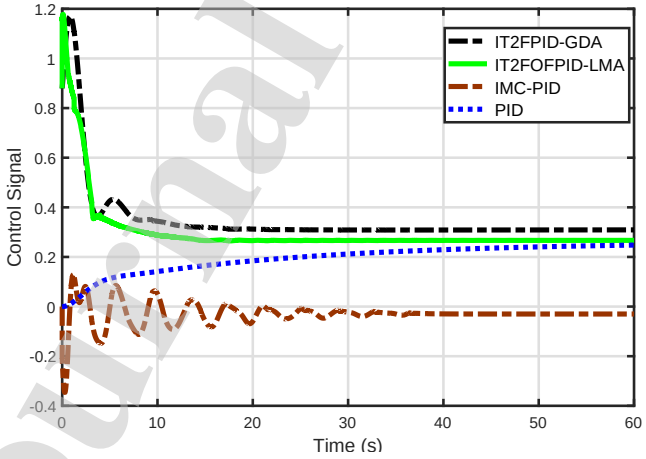

Figure 15: Case 2: Control trajectory without disturbance; area 1

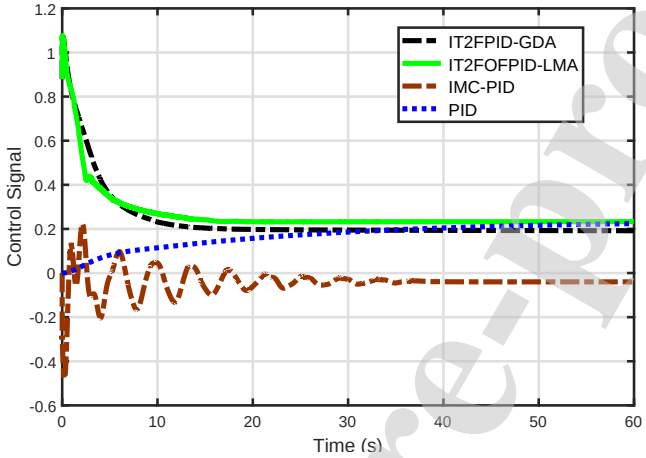

Figure 16: Case 2: Control trajectory without disturbance; area 2

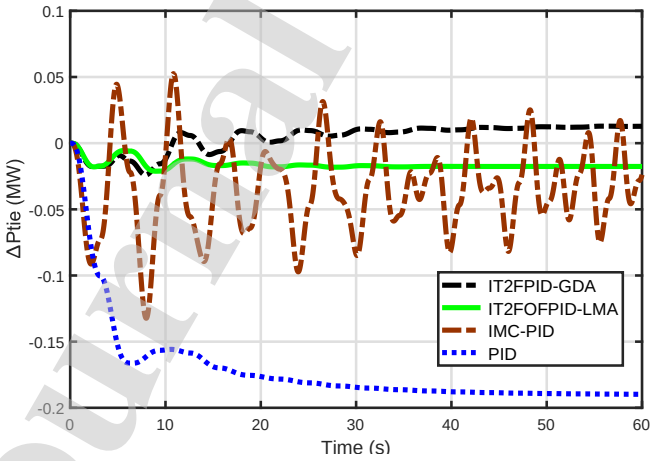

Figure 17: Case 1: Changes of the tie-line power with disturbance

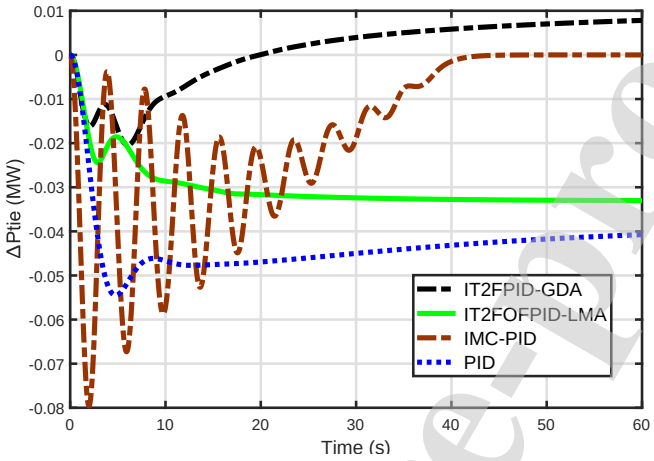

Figure 18: Case 2: Changes of the tie-line power without disturbance

$$ITAE = \int_0^\infty t|e(t)|dt$$

$$ISE = \int_0^\infty e^2(t)dt \tag{43}$$

$$IAE = \int_0^\infty |e(t)|dt$$

In order to investigate the performance, values of ITAE, ISE and IAE measures are represented in both areas for all controllers, and the results are given in Figs. 19 and 20, and Tables 4 and 5.

Table 4: Comparison of performance index values with disturbance (case 1)

Controllers	$ITAE_1$	$ITAE_2$	ISE_1	ISE_2	IAE_1	IAE_2
IT2FPID-GDA	1.759	1.060	0.869	0.4627	0.82360	0.4029
IT2FOFPID-LMA	0.7969	0.280	0.329	0.4830	0.210	0.260
IMC-PID	2.860	1.890	1.279	1.90	1.980	1.679
PID	1.649	0.810	0.5340	1.171	0.890	0.949

Table 5: Comparison of performance index values without disturbance (case 2)

Controllers	$ITAE_1$	$ITAE_2$	ISE_1	ISE_2	IAE_1	IAE_2
IT2FPID-GDA	0.630	1.10	0.70	0.4626	0.6336	0.502
IT2FOFPID-LMA	0.620	0.389	0.150	0.283	0.110	0.1966
IMC-PID	1.8749	0.70	0.890	1.89	0.5526	1.034
PID	0.949	0.7095	0.3348	1.171	0.6646	0.8551

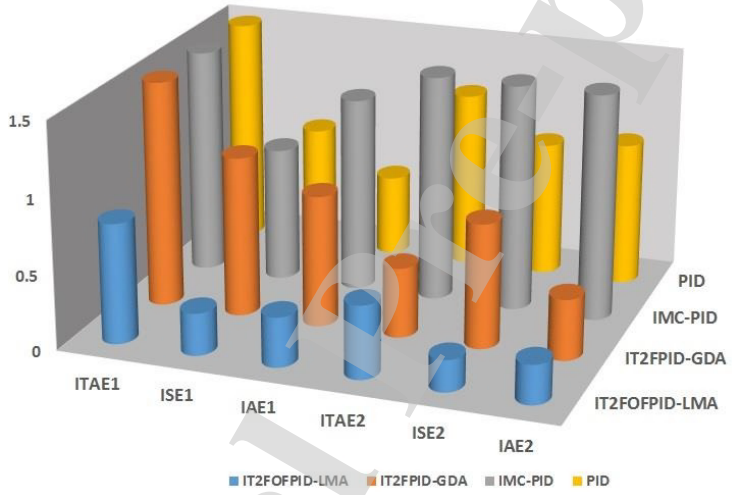

Figure 19: The error integral criteria for areas 1, 2 in case 1

Results of the performance measures show that ITAE changes in our proposed controller are smaller than other controllers. For additional comparison, characteristics of the transient response for the controllers in areas 1 and 3 are listed in Tables 6 and 7. According to Table 6, the overshoot of our proposed controller is 0.61, which is the smallest value among all controllers. Furthermore, by applying a time-varying disturbance at the system output (case 1), minimum overshoot is obtained by our proposed controller which is also better in terms of settling time and rise time.

In order to study the stability of our designed FO controller, Matignon's

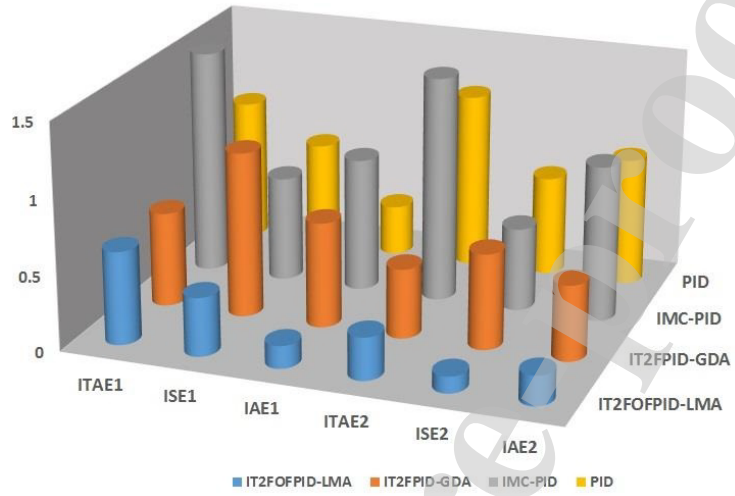

Figure 20: The error integral criteria for areas 1, 2 in case 2

Table 6: Comparison of performance of the system with disturbance (case 1)

Controllers	$T_{s1}(s)$	$T_{s2}(s)$	$T_{r1}(s)$	$T_{r2}(s)$	$OS_1(\%)$	$OS_2(\%)$
IT2FPID-GDA	24	21	0.767	0.438	0.680	0.610
IT2FOFPID-LMA	21	19	0.80	0.794	0.725	0.602
IMC-PID	17	21	0.031	0.161	2.45	1.468
PID	19	23	1.055	1.08	0.526	0.581

stability theorem is used. For a FO system, stability conditions are slightly different. The imaginary diagram is shown in Fig. 21 which is stable for $\alpha = 1$. To demonstrate stability of the proposed controller, Nyquist and Nichols diagrams of the proposed controller are given in Figs. 22 and 23. We see in Fig. 22, the Nyquist diagram does not encircle $(-1, j0)$. According to Nyquist stability theorem $z = n + p$, since n and p are zero, the closed-loop transfer function has no zero on the right plane, and it is stable. Moreover, in the Nichols chart in Fig. 23, the controller bands do not include $(-180°, 0)$ and the system is therefore stable.

Table 7: Comparison of performance of the system without disturbance (case 2)

Controllers	$T_{s1}(s)$	$T_{s2}(s)$	$T_{r1}(s)$	$T_{r2}(s)$	$OS_1(\%)$	$OS_2(\%)$
IT2FPID-GDA	17	18	1.443	1.383	0.6169	0.6759
IT2FOFPID-LMA	15	14	0.901	1.1589	0.739	0.610
IMC-PID	18	19.29	0.540	0.6369	61.70	56.80
PID	26	27.30	13.687	4.044	-2	7.290

We see the trajectory of the output has been converged to the reference trajectory, in finite time, and the control signal has a smooth and reasonable shape with small oscillations.

Consider the following original equation to obtain FOMCON:

$$\begin{cases} a_1 D_t^{n\alpha} y(t) + a_2 D_t^{(n-1)\alpha} y(t) + \ldots + a_n D_t^{\alpha} y(t) + a_{n+1} y(t) = b_1 D_t^{m\alpha} v(t) \\ + b_2 D_t^{(m-1)\alpha} v(t) + \ldots + b_m D_t^{\alpha} v(t) + b_{m+1} v(t) \end{cases} \tag{44}$$

Assuming zero initial condition for input and output signals and calculating the Laplace transform of the above equation, we have:

$$G(s) = \frac{b_1 s^{m\alpha} + b_2 s^{m-1}\alpha + \ldots + b_m s^{\alpha} + b_{m+1}}{a_1 s^{n\alpha} + a_2 s^{(n-1)\alpha} + \ldots + a_n s^{\alpha} + a_{n+1}} \tag{45}$$

Its stability diagram is obtained as in Fig. 21 using the FOMCON toolbox. Such the system is usually known as commensurate order systems.

The transfer function is:

$$FOTF = \frac{324s^{2.8} + 324s^{1.9} + 1200s^{1.8} + 324s + 1200s^{0.9} + 1200}{0.144s^4 + 2.7s^3 + 13.238s^2 + 20.68s + 1} \tag{46}$$

For the practical study, the designed controller is used for LFC of standard 39-bus New England system. This system includes 10 generators, 19 loads, 12 transformers, and 34 transmission lines that are divided into three areas as represented in Fig. 24. Also, conventional power generation (CPG) and loads value are given in Table 8. Stucture of control area $i = 3$ is presented in Fig. 25. The

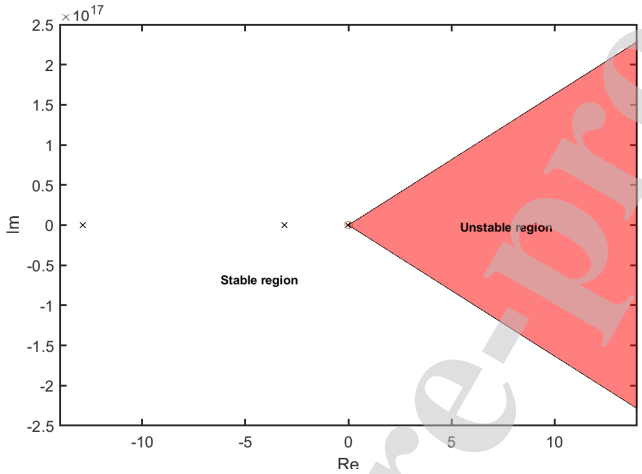

Figure 21: FO system stability region

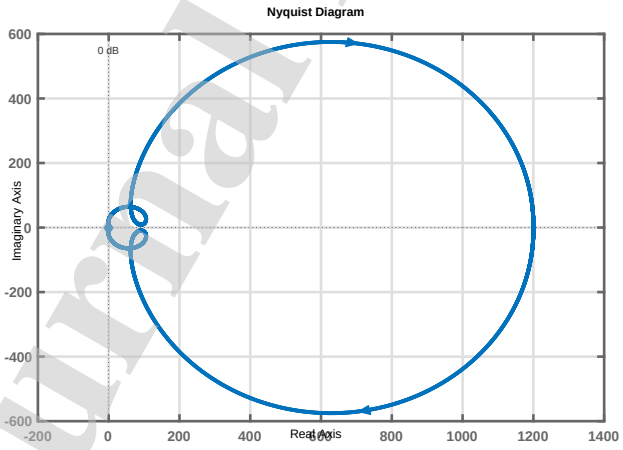

Figure 22: Nyquist diagram for FO system

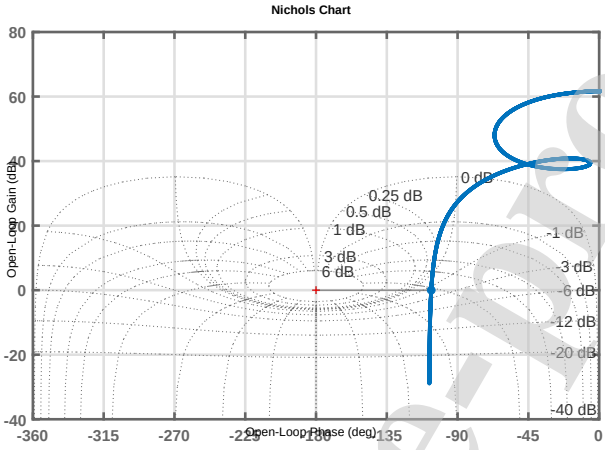

Figure 23: Nichols diagram for FO system

important physical restrictions including generation rate constraint (GRC) and deadband of the governor are considered. In this system, the main simulation parameters of the generator are adopted from [51]. The generators G1, G9 and G4 are responsible for frequency in the areas 1, 2 and 3, respectively. For more comparison, the T1FIS is designed and frequency changes of the designed controller in three areas are compared with that of the T1FIS, and the results are shown in Figs. 26-28. The T1FIS if-then rules are given in Table 9, where we use Negative (N), Positive (P), Zero (Z), Medium (M) and Small (S).

The literature review demonstrates that researchers have selected in general 0.01 step load disturbance, but in this paper, a step load increasing of 0.9 p.u. at areas 1 and 3 is considered with nonlinear constraints. As shown in Figs. 26-28, when our proposed controller is used, settling time is shorter than T1FIS. Also, we see from deviation responses that the overshoot is large in case of T1FIS. Despite the restrictions and nonlinearities of the power system, our proposed method outperforms the T1FIS in all three areas. Also, the proposed controller results are found to be satisfactory despite the disturbance.

Table 8: Conventional power generation and loads values in areas 1-3

	Area		
	1	2	3
CPG	134.570 MW	106.381 MW	163.90 MW
Loads	329.249 MW	74.0510 MW	182.010 MW

Table 9: If-then rules for T1FIS

ACE	ΔACE	K_p	K_i
N	P	M	S
N	Z	M	S
N	N	S	M
Z	N	S	S
Z	Z	S	H
Z	P	S	S
P	N	S	S
P	Z	S	S
P	P	M	S

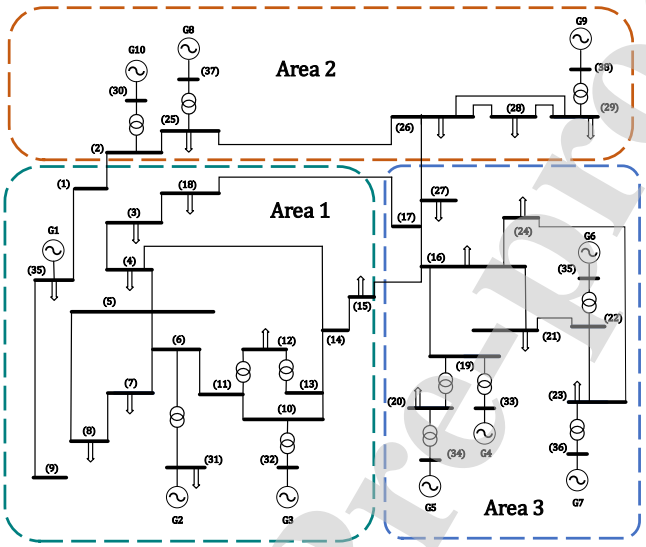

Figure 24: Single-line diagram of 39-bus power system

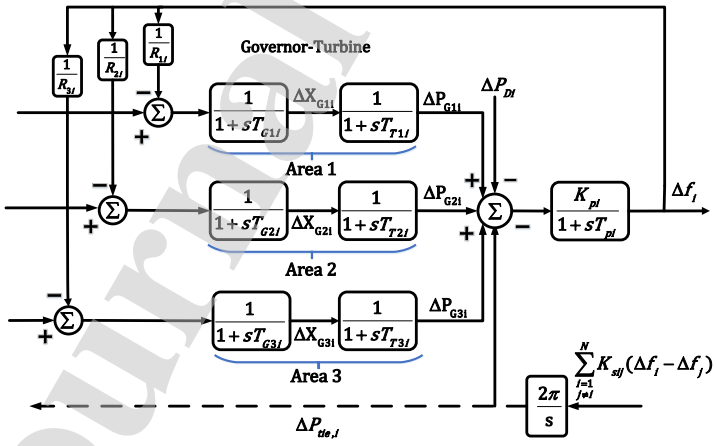

Figure 25: Block diagram of control area $i = 3$

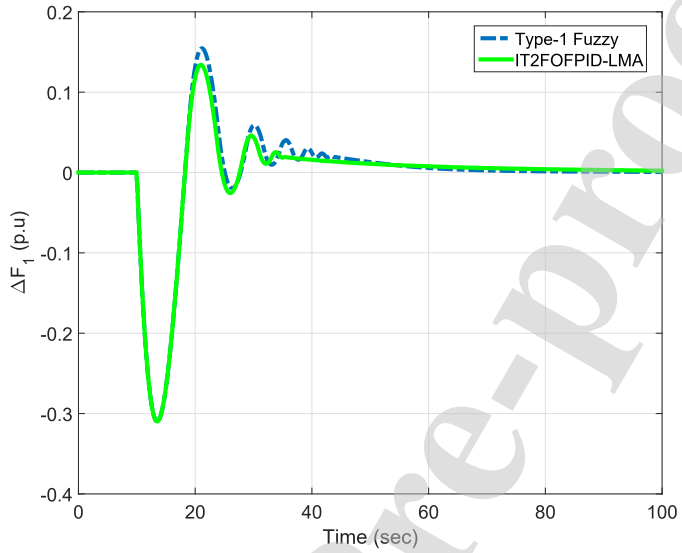

Figure 26: Frequency changes for the New England test system; area 1

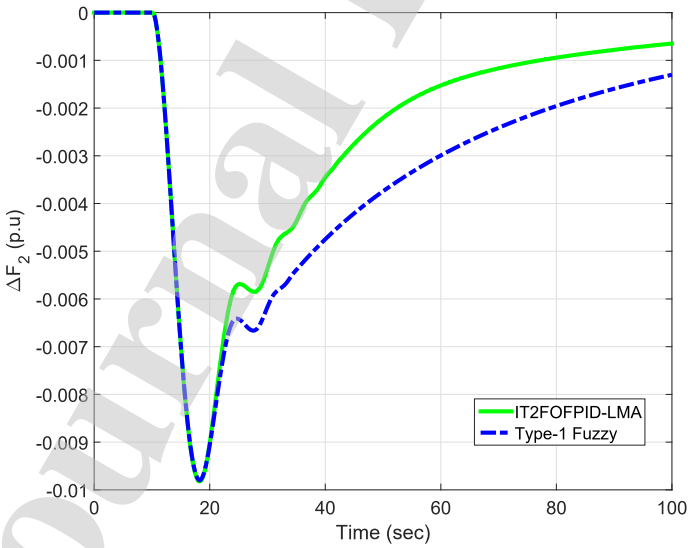

Figure 27: Frequency changes for the New England test system; area 2

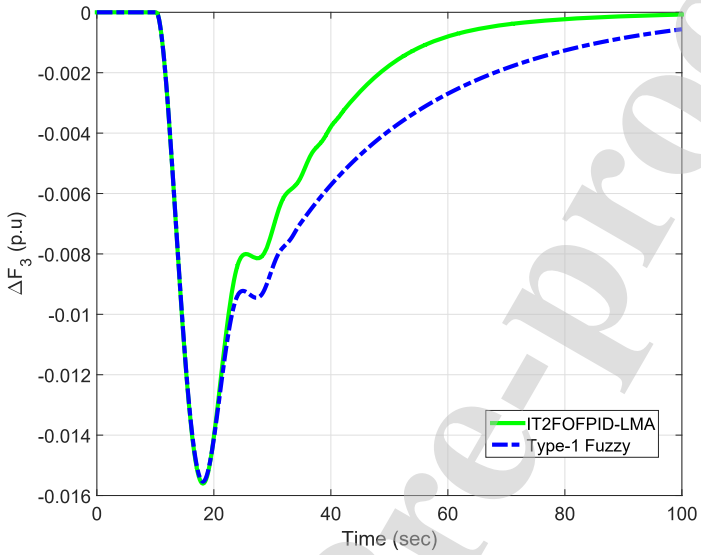

Figure 28: Frequency changes for the New England test system; area 3

7. Conclusions

For performance improvement and robustness of power systems against frequency fluctuations caused by load changes, a new FO fuzzy method is proposed. For reducing sensitivity to parameter changes of the system, system dynamics are considered to be unknown, and MLP-NN is used to obtain Jacobian of the approximation model. IT2FIS is used to model the uncertainty, and fuzzy parameters are trained using LMA, which has better efficiency and performance in terms of speed and robustness compared to similar methods.

Simulation results show that our proposed controller improves the performance of the control system significantly by tuning parameters of the control system. Since IT2FIS has more adjustable parameters, it thus improves system efficiency; also, it is proper for uncertainties and slow speed is compensated by training the LMA. The proposed IT2FOFPID-LMA is compared with IT2FPID-GDA, IMC-PID and PID controllers, and a time-varying disturbance is applied

at the output to study the robustness of our proposed method. Error integral criteria is used for assessment. The main limitation of the proposed control system in practical applications is its more complexity in contrast to another simple controller such as PID. To show the effectiveness of the designed controller on practical application, the New England 39-bus test system is used. A comparative study among T1FIS and our proposed controllers is carried out in this paper by considering 0.9 p.u. step load changes in areas 1 and 2. Simulations verifies that our designed controller is better and more robust compared to the other controllers. For future studies, the designed control method will further be tested for even larger-scale test systems by considering demand response programs and the impact of existing large-scale wind turbines in the LFC of a multi-area power system. Also, Mittag-Leffler stability is investigated in our future studies.

References

[1] Debbarma S and Dutta A, Utilizing electric vehicles for lfc in restructured power systems using fractional-order controller, IEEE Transaction on Smart Grid 8 (6) (2017) 2554 – 2564. doi:10.1109/TSG.2016.2527821.

[2] Velusami S and Chidambaram I.A, Decentralized biased dual-mode controllers for load frequency control of interconnected power systems considering gdb and grc non-linearities, Energy Convers. Manag 48 (2007) 1691–1702. doi:10.1016/j.enconman.2006.11.003.

[3] Arivoli R and Chidambaram I.A, Cpso based lfc for a two-area power system with gdb and grc nonlinearities interconnected through tcps in series with the tie-line, Int. J. Comput. Applications 38 (7) (2012) 1–10. doi:10.1109/TSG.2016.2527821.

[4] Arya Y and Kumar N, Design and analysis of bfoa-optimized fuzzy pi/pid controller for agc of multi-area traditional/restructured electrical

ower systems, Soft Computing 21 (2017) 6435—-6452. doi:10.1007/s00500-016-2202-2.

[5] Kumar Sahu R, Sekhar Gorripotu T and Panda S, Sekhar gorripotu t, panda s. a hybrid de–ps algorithm for load frequency control under deregulated power system with upfc and rfb, Ain Shams Engineering Journal 8 (6) (2015) 893—-911. doi:10.1016/j.asej.2015.03.011.

[6] Lin Da, Wang X, Nian F and Zhang Y, Dynamic fuzzy neural networks modeling and adaptive backstepping tracking control of uncertain chaotic systems, Neurocomputing 73 (6) (2010) 2873–2881. doi:10.1016/j.neucom.2010.08.008.

[7] Bhavanisankar Ch and Sudha K. R, An adaptive technique to control the load frequency of hybrid distributed generation systems, Soft Computing 23 (2019) 12385—-12400. doi:10.1007/s00500-019-03779-w.

[8] Juang C-F and Lu C-F, Load-frequency control by hybrid evolutionary fuzzy pi ontroller, Proc. Inst. Electr. Eng. Gener, Transm. Distrib 153 (2006) 196—204.

[9] MAS A, MF A and HT D, Design of aerospace control systems using fractional pid controller, Adv Res 3 (3) (2012) 225–232. doi:10.1007/s00500-016-2202-2.

[10] Hamamci SE, An algorithm for stabilization of fractional-order time delay systems using fractional-order pid controllers, IEEE Trans Automatic Control 52 (10) (2007) 1964–1969. doi:10.1109/TAC.2007.906243.

[11] Jia L, Xiuyuna M and Zaozhena L, Freestyle fractional-order controller design with pso for weapon system, ESEP Singapore 13 (2011) 7577–7582. doi:10.1016/j.egypro.2011.12.491.

[12] Zamani M, Karimi-Ghartemani M, Sadati N and Parniani M, Design of fractional-order pid controller for an avr using particle swarm optimiza-

tion, Control Eng Practice 17 (12) (2009) 1380—-1387. doi:10.1016/j.conengprac.2009.07.005.

[13] Tang Y, Cui M, Hua Ch, Li L and Yang Y, Optimum design of fractional-order pikdl controller for avr system using chaotic ant swarm, Expert Syst Appl 39 (8) (2012) 6887–6896. doi:10.1016/j.conengprac.2009.07.005.

[14] Kumar A and Kumar V, A novel interval type-2 fractional order fuzzy pid controller: Design. performance evaluation, and its optimal time domain tuning, ISA Trans 68 (2017) 251–275. doi:10.1016/j.isatra.2017.03.022.

[15] Pan I and Das S, Chaotic multi-objective optimization based design of fractional-order pikdl controller in avr system, Int J Electr Power Energy Syst 43 (1) (2012) 393—-407. doi:10.1016/j.ijepes.2012.06.034.

[16] Maiti D, Acharya A, Chakraborty M, Konar A and Janarthanan R, Tuning pid and pikdl controllers using the integral time absolute error criterion, In: Proceedings IEEE international conference on information and automation for sustainability (2008).

[17] Biswas A, Das S, Abraham A and Dasgupta S, Design of fractional-order pikdl controllers with an improved differential evolution, Eng Appl Artif Intell 22 (2009) 343–350. doi:10.1016/j.isatra.2017.03.022.

[18] Monje CA, Vinagre BM, Chen YQ, Feliu V, Lanusse P and Sabatier J, Proposals for fractional pikdl tuning, In: Fractional differentiation and its applications. Bordeaux 43 (1) (2004) 393—-407.

[19] Vale´rio D and Costa JS. da, Tuning of fractional pid controllers with ziegler–nichols type rules, Signal Process 86 (10) (2006) 2771–2784.

[20] Zhao Ch, Dingy UX and Chen Y, A fractional-order pid tuning algorithm for a class of fractional-order plants, IEEE Int Conf Mech Automatl 1 (2005) 216—-221. doi:10.1109/ICMA.2005.1626550.

[21] Pan I and Das S, Fractional-order fuzzy control of hybrid power system with renewable generation using chaotic pso, ISA Trans 62 (2016) 19–29.

[22] Asgharnia A, Shahnazi A and Jamali A, Performance and robustness of optimal fractional fuzzy pid controllers for pitch control of a wind turbine using chaotic optimization algorithms, ISA Trans 79 (10) (2018) 393–407.

[23] Dokht Shakibjoo A, Moradzadeh M, Moussavi SM and Afrakhte H, Online adaptive type-2 fuzzy logic control for load frequency of multi-area power system., Journal of Intelligent & Fuzzy Systems 37 (2019) 1033–1042. doi:10.3233/JIFS-181963.

[24] Dokht Shakibjoo A, Moradzadeh M, Moussavi SZ and Vandevelde L, A novel technique for load frequency control of multi-area power systems, Energies 13 (2020) 2125. doi:10.3390/en13092125.

[25] Mohammadzadeh A and Kayacan E, A novel fractional-order type-2 fuzzy control method for online frequency regulation in ac microgrid, Engineering Applications of Artificial Intelligence 90 (2020) 103483. doi:10.1016/j.engappai.2020.103483.

[26] Nagendra K, Barjeev T and Vishal K, Application of fractional order pid controller for agc under deregulated environment, International Journal of Automation and Computing 15 (2018) 88–93. doi:10.1007/s11633-016-1036-9.

[27] Chen YQ, Fractional order control-a tutorial, International Journal of Automation and Computing (2009) 1398–1411.

[28] Ruano A, Cabrita C, Oliveira J, Tikk D and Koczy L, Supervised training algorithms for b-spline neural networks and fuzzy systems, In IFSA World Congress and 20th NAFIPS International Conference 5 (2001) 2830 –2835.

[29] Yong P and Guo-hua L, A fuzzy optimization neural network model using second order information in fuzzy systems and knowledge discovery, FSKD '09. Sixth International Conference 4 (2009) 221–227.

[30] Palit A and Babuska R, Efficient training algorithm for takagi-sugeno type neuro-fuzzy network in fuzzy systems, The 10th IEEE International Conference 3 (2001) 1367–1371.

[31] Sondhi S and Hote YV, Efficient training algorithm for takagi-sugeno type neuro-fuzzy network in fuzzy systems., Fractional-order controller and its applications: a review. In: Proc. of Asia MIC, Phuket, Thailand 3 (2012) 1367– –1371.

[32] Abdon A, Fractional operators with constant and variable order with application to geo-hydrology, ScienceDirect 3 (2018) 79–112. doi:10.1016/B978-0-12-809670-3.00005-9.

[33] Podlubny I, Fractional differential equations, San Diego: Academic Press (1999).

[34] Oldham KB and Spanier J, The fractional calculus: Theory and application of differentiation and integration to arbitrary order, Academic Pres. New York (1974).

[35] Abdon A, Fractional order pid controller for load frequency control, energy conversion and management, ScienceDirect 3 (2018) 79–112. doi:10.1016/B978-0-12-809670-3.00005-9.

[36] Khanesar MA, Teshnehlab M, Kayacan E and Kaynak O, A novel type-2 fuzzy membership function: application to the prediction of noisy data, in: IEEE Inter-national Conference on Computational Intelligence for Measurement Systems and Applications 3 (2010) 128—-133.

[37] Bevrani H, Robust power system frequency control, Springer US 30 (2010) 79–112. doi:10.1007/978-0-387-84878-5.

[38] Sabahi K, Ghaemi S and Pezeshki S, Application of type-2 fuzzy logic system for load frequency control using feedback error learning approaches, Applied Soft Computing 21 (2014) 1–11. doi:10.1016/j.asoc.2014.02.022.

[39] Mendel JM, Uncertain rule-based fuzzy logic system: Introduction and new directions, Upper Saddle River, Prentice Hall 21 (2001) 1–11.

[40] Castillo O and Melin P, Type-2 fuzzy logic: Theory and applications, springer (2008). doi:10.1007/978-3-540-76284-3.

[41] Wilamowski BM and David Irwin J, Intelligent systems, CRC Press Taylor & Francis Group (2011).

[42] Khanesar M. A, Kayacan E, Teshnehlab M and Kaynak O, Levenberg marquardt algorithm for the training of type-2 fuzzy neuro systems with a novel type-2 fuzzy membership function, IEEE Symposium on Advances in Type-2 Fuzzy Logic Systems (2011) 88–93.

[43] Cong Chen T, Jian Han D, Au F and Tham L, Acceleration of levenberg-marquardt training of neural networks with variable decay rate, In Neural Networks, Proceedings of the International Joint Conference 3 (2003) 1873–1878.

[44] Zhang H, Wang X-Y and Lin X-H, Topology identification and module–phase synchronization of neural network with time delay, IEEE Transactions on Systems. Man, and Cybernetics: Systems 47 (6) (2017) 885–892. doi:10.1109/TSMC.2016.2523935.

[45] Mohammadzadeh A and Ghaemi S, Optimal synchronization of fractional-order chaotic systems subject to unknown fractional order, input nonlinearities and uncertain dynamic using type-2 fuzzy CMAC, Nonlinear Dynamics 88 (4) (2017) 2993–3002. doi:10.1007/s11071-017-3427-z.

[46] Mohammadzadeh A and Ghaemi S, Optimal synchronization of fractional-order chaotic systems subject to unknown fractional order, input nonlinearities and uncertain dynamic using type-2 fuzzy cmac, input nonlinearities and uncertain dynamic using type-2 fuzzy CMAC, Nonlinear Dynamics 88 (4) (2017) 2993–3002. doi:10.1007/s11071-017-3427-z.

[47] Widodo W and Handri D, Improving levenberg-marquardt algorithm inversion result using singular value decomposition, Earth Science Research 5 (2016) 2993–3002. doi:10.5539/esr.v5n2p20.

[48] Lin D and Wang X, Self-organizing adaptive fuzzy neural control for the synchronization of uncertain chaotic systems with random-varying parameters, Neurocomputing 74 (2011) 2241–2249. doi:10.1016/j.neucom.2011.03.003.

[49] Tan W, Unified tuning of pid load frequency controller for power systems via imc, IEEE Trans. Power Syst 25 (2010) 341—-350. doi:10.1109/TPWRS.2009.2036463.

[50] Report I.C, Dynamic models for steam and hydro turbines in power system studies, IEEE Trans. Power Syst 25 (1973) 1904–1915. doi:10.1109/TPAS.1973.293570.

[51] Bevrani H, Daneshfar F and Daneshmand R.P, Intelligent power system frequency regulations concerning the integration of wind power units, Springer, Berlin, Heidelberg 0 (2010). doi:10.1007/978-3-642-13250-6_15.

Highlights

- A new simple fractional-order type-2 fuzzy control system is proposed for LFC.
- The dynamics of the plant are assumed to be uncertain.
- The parameters of the fuzzy controller are tuned based on the Levenberg-Marquardt algorithm (LMA).
- Unlike the other similar methods, the Jacobian of the plant is not required.
- The proposed controller produces better performance as compared to the other three controllers.

Declaration of interests

☒ The authors declare that they have no known competing financial interests or personal relationships that could have appeared to influence the work reported in this paper.

☐The authors declare the following financial interests/personal relationships which may be considered as potential competing interests: